Revisiting the validity of Braak's equation on altitudinal temperature lapse rate using thermal-infrared bands of Landsat 8

Desi Suyamto, Lilik Prasetyo, Yudi Setiawan

Desi Suyamto, Lilik Prasetyo, Yudi Setiawan, "Revisiting the validity of Braak's equation on altitudinal temperature lapse rate using thermal-infrared bands of Landsat 8," Proc. SPIE 10773, Sixth International Conference on Remote Sensing and Geoinformation of the Environment (RSCy2018), 107730B (6 August 2018); doi: 10.1117/12.2325356

SPIE.

Event: Sixth International Conference on Remote Sensing and Geoinformation of the Environment (RSCy2018), 2018, Paphos, Cyprus

Revisiting the validity of Braak's equation on altitudinal temperature lapse rate using thermal-infrared bands of Landsat 8

Desi Suyamto*, Lilik Prasetyo and Yudi Setiawan
Forests 2020, Environmental Analysis and Spatial Modelling Laboratory, Department of Forest Resource Conservation, Faculty of Forestry, Bogor Agricultural University, Bogor, Indonesia

ABSTRACT

Spatial data on temperature are of importance to the studies concerning the roles of climate, including the impacts of climate change on ecosystem functions and ecosystem services. However, most temperature data are available at station level, sparsely and irregularly distributed across space as points, and the accuracies of spatial-interpolation-based surface models decrease with decreasing density of the observation points. Meanwhile, relationship between elevation and temperature has been acknowledged, which basis is grounded in thermodynamics theory by Robert Clausius, and later known as altitudinal temperature lapse rate. Most studies related to altitudinal temperature lapse rate in Indonesia have been using and scaling-up the findings from Cornelis Braak, based on his research in Java during the 1920s. According to Braak, temperature decreases by 0.60°C and 0.55°C as the elevation increases by 100 m asl, for areas below and above 1500 asl, respectively. With regards to climate change, Braak's findings should be updated, since it determines climatic geo-data, used for strategic geo-planning (e.g. for suitability mapping). Thus, in this respect, the study is aimed at revisiting altitudinal temperature lapse rates in Indonesia using thermal-infrared bands of Landsat 8. With regards to Braak's observation stations, one window area in Bogor, West Java, Indonesia was selected as the study site. The results suggest that altitudinal temperature lapse rate decreased from 0.0016 to 0.0021^{o}C.m^{-1}, as compared to Braak's equation, which indicate significant temperature increase. The results also suggest that temperature increase in the window area was about 1.58^{o}C, doubled from temperature increase at global scale of about 0.8 ^{o}C, which implies to losses of montane and sub montane zones according to Holdridge life zone of about 7 km^2 (100%) and 727 km^2 (32.53%), respectively; and gain of basal zone of about 734 km^2 (211.77%).

Keywords: Altitudinal temperature, Braak, climate change, Holdridge life zone, Landsat 8, thermal-infrared

1. INTRODUCTION

Spatial data on temperature are of importance to the studies concerning the roles of climate, including the impacts of climate change on ecosystem functions and ecosystem services [1]; [2]; [3]; [4]; [5]. In fact, most temperature data are available at station level, sparsely and irregularly distributed across space as points [6]. Estimated density of observation stations measuring temperature in Indonesia, based on spatial distribution of 178 stations located in each Technical Implementation Unit (UPT) of Indonesian Agency for Meteorology, Climatology and Geophysics (BMKG) is about 36 stations per grid, with a grid size of 0.1º x 0.1º (approximately 121 km^2), ranging from 32 to 95 stations per grid, with Euclidean distance between stations of about 1,670 km, ranging from 0.01 to 5,246 km (Figure 1). Meanwhile, spatial interpolation of low density points decreases the accuracy of generated surface model [7]; [8]. Moreover, [7] reported that deformations across surface model due to spatial interpolation of measurement points with densities of 14.3 points/100 m^2 and 0.3 points/100 m^2 were about 1.06 m and 2.51 m, respectively. Thus, accuracy of spatial-interpolation-based surface models decreases with decreasing density of the observation points. It implies that accuracies of surface temperature models generated using spatial interpolation based on observation stations with density of about 36 stations/121 km^2 are therefore scientifically not acceptable.

In fact, relationship between elevation and temperature has been acknowledged, which basis is grounded in thermodynamics theory by Robert Clausius [9]. In the troposphere, temperature decreases at overall lapse rate of about 6.5ºC/km, ranging from 5 to 7 ºC/km, with diurnal and seasonal variations in higher latitudes [10]. Surface temperature model developed based on temperature lapse rate and digital elevation model (DEM) was reported to have relatively

*d_suyamto@apps.ipb.ac.id; phone 62 251 8621677; forests2020.ipb.ac.id

Sixth International Conf. on Remote Sensing and Geoinformation of the Environment (RSCy2018),
K. Themistocleous, G. Papadavid, S. Michaelides, V. Ambrosia, D. G. Hadjimitsis, Eds., Proc. of SPIE Vol. 10773,
107730B · © 2018 SPIE · CCC code: 0277-786X/18/$18 · doi: 10.1117/12.2325356

high accuracy [6]. However, most studies related to altitudinal temperature lapse rate in Indonesia have been using and scaling-up the findings from Cornelis Braak, based on his research in Java during the 1920s [11].

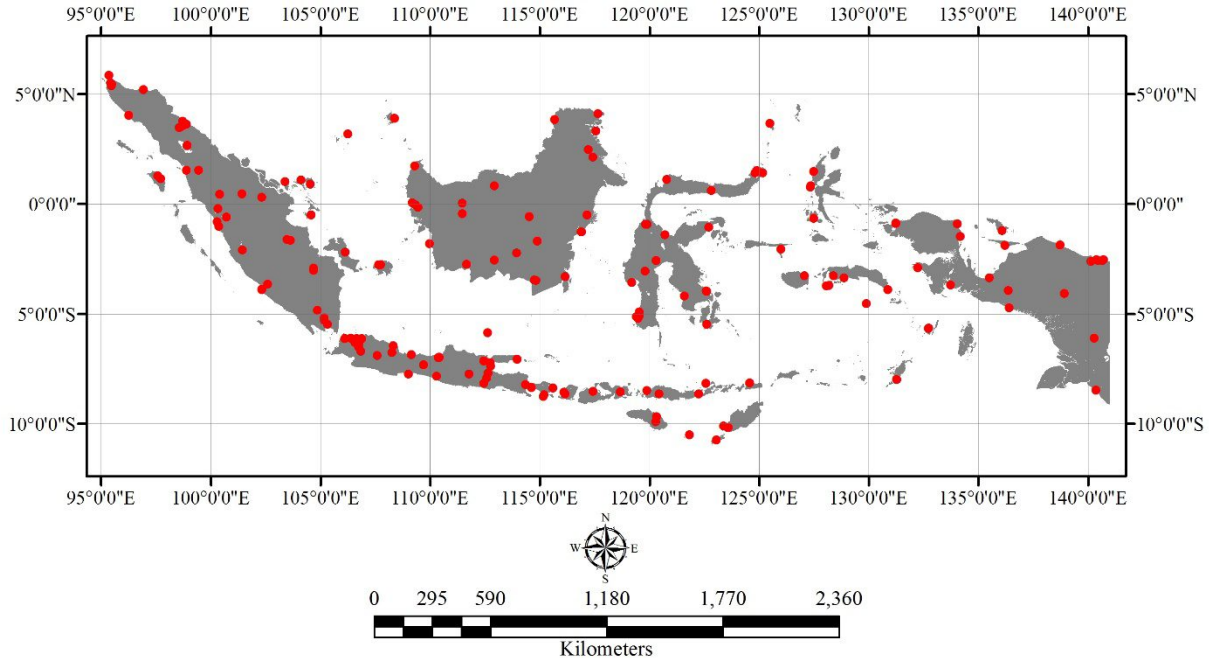

Figure 1. Spatial distribution of 178 observation stations measuring temperature located in each technical implementation unit of BMKG (red points). Point geodata source: http://dataonline.bmkg.go.id.

Based on published scientific works of 1975-2017 period, we identified 28 studies applying Braak's equation, ranging from local scale to regional scale (i.e. Southeast Asia), with various purposes, i.e. for estimating cloud height based on temperature difference between cloud and land surface [12]; for bioclimatic analysis in developing ecological guidelines for land development and management of humid tropical forest environments [13]; for assessing biodiversity on species distribution and abundance of montane to sub-alpine zones [14]; for drought analysis [15]; for ecosystem change study [16]; for epidemiology analysis of dengue fever [17]; for landscape planning [18]; for rice crop modelling [19]; and for land suitability analyses for agricultural cropping systems, forestry/tree-based planting systems, and animal husbandry (e.g [20] and 19 similar studies by others).

According to Braak's equation, temperature decreases by 0.60°C and 0.55°C as the elevation increases by 100 m asl, for areas below and above 1500 asl, respectively [21]. With regards to climate change, Braak's findings should be updated, since it determines climatic geodata, used for strategic geo-planning (e.g. for suitability mapping). Meanwhile, satellite technology with sensors sensitive in the thermal-infrared (TIR) wavelength (around 3-50 μm) is capable of monitoring current temperature at the land surface [22]. Thus, in this respect, the study is aimed at revisiting altitudinal temperature lapse rates in Indonesia based on Braak's equation using TIR bands of Landsat 8. With regards to Braak's observation stations, one window area in Bogor, West Java, Indonesia was selected as the study site. Validity of Braak's equation with regards to the current climatic condition was evaluated and its implication for relevant geo-planning was assessed.

2. WINDOW AREA AND DATA

2.1 Window area

A site situated around Mount Halimun-Salak and Mount Gede-Pangrango, Bogor, West Java, Indonesia was selected as the window area to evaluate altitudinal temperature lapse rate (Figure 2).

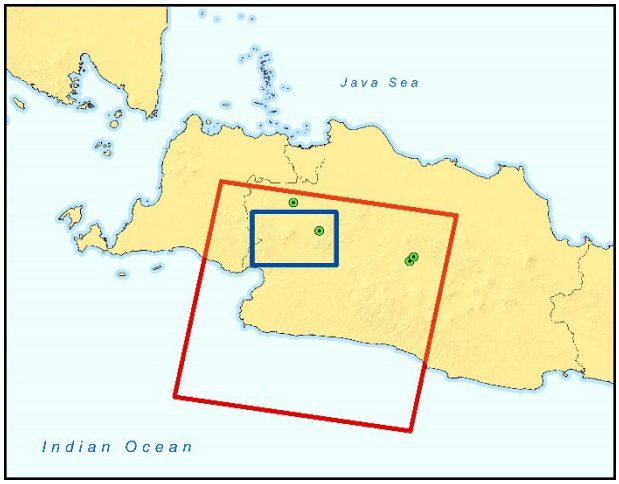

Figure 2. Window area of the study (blue line), situated around Mount Halimun-Salak and Mount Gede-Pangrango, Bogor, West Java, Indonesia, as subset of Landsat 8 path/row 122/65 (red line), where green circles are the locations of climatological stations used to calibrate the estimated LST.

2.2 Data

Landsat 8 imageries path/row 122/65 acquired on 9 June 2014 and 23 February 2016, with regards to minimum cloud cover; ground temperature data from 4 available observation stations of the same acquisition dates of Landsat 8 imageries; and SRTM DEM on 30 m grid resolution were used as input data in this study (Table 1). In this case, blue band (bands 2) of Landsat 8 was used for cloud and cloud shadow masking, red and NIR bands (bands 4 and band 5) were used for estimating land surface emissivity (LSE), and TIR bands (bands 10 and band 11) were used for estimating top of atmosphere brightness temperature (BT). Meanwhile, ground temperature data and SRTM DEM were used for calibrating LST and performing elevation-temperature correlation analyses in order to update altitudinal temperature lapse rate equation. The main tool for data analyses used in this study was ArcGIS 10.2.2.

Table 1. Input data used for the analyses.

Data	Acquisition date	Source
Landsat 8 of path/row 122/65, bands: 2 (blue), 4 (red), 5 (NIR), 10 (TIR) and 11 (TIR)	9 June 2014 and 23 February 2016	https://earthexplorer.usgs.gov
SRTM-DEM at resolution of 30-m	-	https://gdex.cr.usgs.gov
Ground temperature data from 4 available observation stations	9 June 2014 and 23 February 2016	http://dataonline.bmkg.go.id

3. METHODS

Methods of this study comprise two main work flows: (i) work flow to update altitudinal temperature lapse rate based on current climatic condition of estimated LST; and (ii) work flow to map altitudinal Holdridge life zone based on elevation-based surface temperature maps, estimated using both Braak's equation and updated altitudinal temperature lapse rate equation; in order to assess implication of possible shift of altitudinal temperature lapse rate of the current climatic condition from Braak's equation due to climate change on altitudinal Holdridge life zone.

3.1 Updating altitudinal temperature lapse rate

Work flow to update altitudinal temperature lapse rate comprises 7 main steps (Figure 3). First of all, cloud and cloud shadow masking was carried out based on iso cluster unsupervised classification using band 2 of Landsat 8 with number of classes of 4 at 100 iterations; where class 1 (the brightest) was determined as cloud and class 4 (the darkest) was determined as cloud shadow. The resulted cloud and cloud shadow mask was used for cloud and cloud shadow removal within bands 4, 5, 10, and 11.

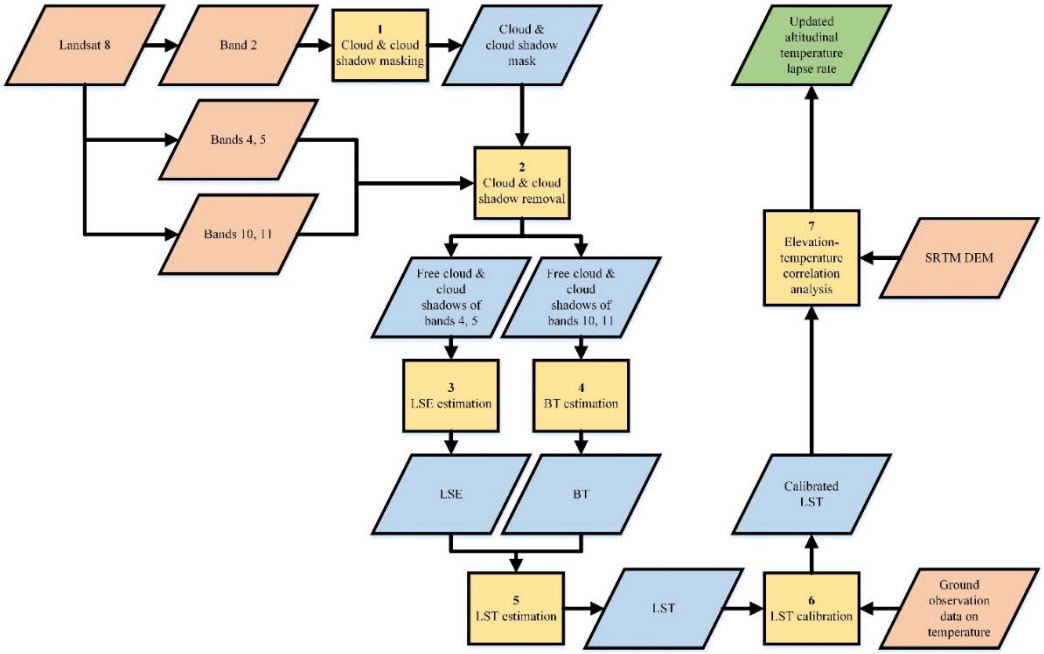

Figure 3. Work flow to update altitudinal temperature lapse rate.

Based on cloud-and-cloud-shadow-free of bands 4 and 5, LSE (dimensionless) was estimated based on equation adopted from [23]:

$$LSE = 0.004\left(\frac{NDVI - NDVI_{min}}{NDVI_{max} - NDVI_{min}}\right)^2 + 0.986 \quad (1)$$

Based on cloud-and-cloud-shadow-free of bands 10 and 11, BT of each TIR band (°K) was estimated based on equation adopted from [24]:

$$BT = \frac{K_2}{ln\left(\frac{K_1}{M_L DN + A_L}\right) + 1} \quad (2)$$

In this case, K_1 and K_2 denote band-specific thermal conversion constants – available from Landsat 8 metadata; M_L and A_L denote band-specific multiplicative and additive rescaling factors respectively – both available from Landsat 8 metadata; and DN denotes digital number of pixels.

Based on LSE and BT, LST (°C) was estimated based on modified radiative transfer equation from [25]:

$$LST = \frac{BT_{average}}{1 + \frac{\lambda}{p} BT_{average} . \ln(LSE)} - 273.15 \quad (3)$$

Where, $BT_{average}$ is the average of estimated BTs based on bands 10 and 11; λ is the mean of TIR wavelength of Landsat 8 sensors (10.89 μm); and p is a constant with value of 14,380 m°K, calculated from: $\frac{Planck\ constant\ x\ light\ velocity}{Boltzmann\ constant}$.

The estimated LST was later calibrated using ground temperature data. Finally, the updated altitudinal temperature lapse rate equation was developed based on elevation-temperature correlation analyses. In this case, elevation was classified at

100-m class interval following Braak's methodology [21] and temperature data were averaged from LST of random points located at each elevation class.

3.2 Mapping altitudinal Holdridge life zone

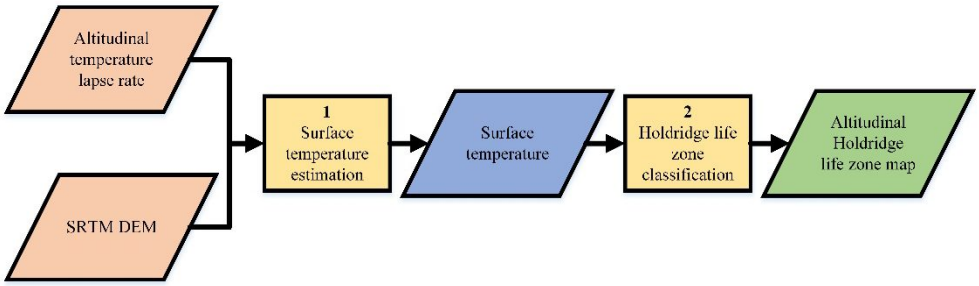

Figure 4. Work flow to map altitudinal Holdridge life zone based on elevation-based surface temperature map.

Figure 4 illustrates the work flow for assessing the implication of possible shift of altitudinal temperature lapse rate of the current climatic condition from Braak's equation due to climate change on altitudinal Holdridge life zone. First of all, land surface temperature maps were generated based on SRTM DEM using altitudinal temperature lapse rate equation:

$$T_z = T_0 - LR.z \quad (4)$$

Where, T_z and T_0 are land surface temperature (°C) at elevation z m asl and elevation zero m asl, respectively; LR is temperature lapse rate (°C.m^{-1}); and z is elevation (m asl). In this case, according to Braak (1929), T_0=26.3 °C; while LR=0.0060°C.m^{-1} and 0.0055°C.m^{-1} for elevation < 1500 m asl and ≥ 1500 m asl, respectively.

Finally, altitudinal Holdridge life zone was classified into 6 categories based on criteria as follows [4]: (i) basal, if land surface temperature is higher than 24°C; (ii) sub montane, if land surface temperature is between 12-24°C;`(iii) montane, if land surface is between 6-12°C; (iv) sub alpine, if land surface is between 3-6°C; and (v) alpine, if land surface is between 1.5-3°C; and (vi) nival, if land surface is lower than 1.5°C.

4. RESULTS AND DISCUSSIONS

4.1 LST calibration

Figure 5 shows the estimated LST based on TIR bands of Landsat 8 acquired on 9 June 2014 and 23 February 2016; where underestimation of LST was found mostly in northern part of LST map from the year 2016 (see blue color in the LST maps), due to appearance of relatively large haze on 23 February 2016 in the northern part (see dark color in the panchromatic maps of band 10). However, locations of the observation stations for calibration and the window area for further analyses were outside the underestimated LST zones (see black stars and black rectangles in the LST maps). Moreover, Figure 6 shows correlation between estimated LST and observed ground temperature, which linear regression, y=1.3827x-7.8878 with r^2=0.9539, was used for calibration.

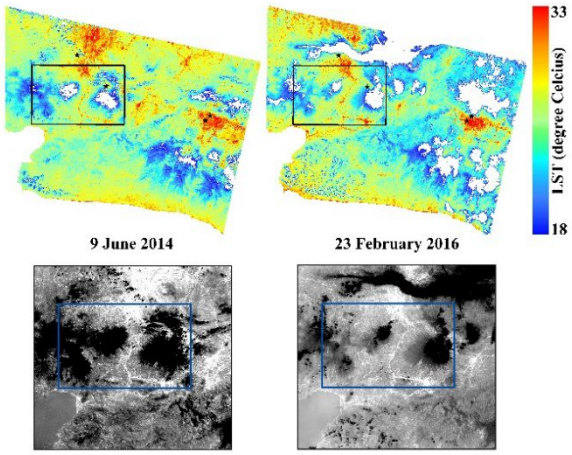

Figure 5. Estimated LST based on TIR bands of Landsat 8 acquired on 9 June 2014 and 23 February 2016 (top) and their panchromatic TIR bands, i.e. band 10 (bottom). Stars indicate locations of observation stations, and rectangles indicate the window area of this study.

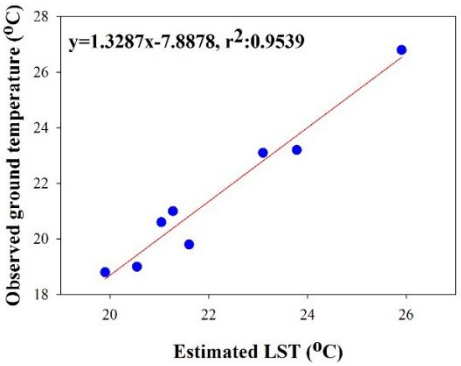

Figure 6. Linear regression between estimated LST and observed ground temperature used for calibration.

4.2 Updated altitudinal temperature lapse rate

Calibrated LST data from 16,313 random points were averaged according to elevation classes at 100-m interval (blue crosses in Figure 7). Linear regression between average LST and mid values of each elevation class interval was used to update the temperature lapse rate equation (red line in Figure 7). Comparing the slopes of the updated lapse rate and Braak's lapse rate at the same intercept, i.e. 26.3°C (green and purple lines in Figure 7), it is obvious that the updated altitudinal temperature lapse rate decreased from 0.0016 to 0.0021°C.m^{-1}, which indicate significant temperature increase.

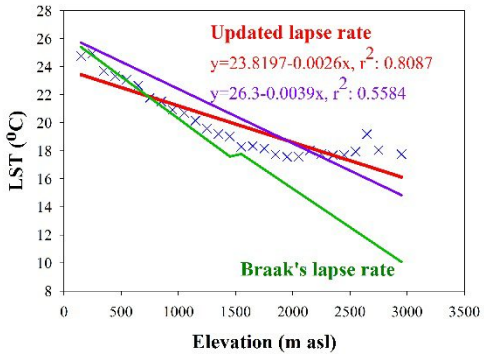

Figure 7. Updated altitudinal temperature lapse rate (red line), as linear regression between elevation and average temperature of 16,313 random points (blue crosses), compared to Braak's lapse rate (green line). In this case, to be comparable with Braak's lapse rate, the intercept of the updated lapse rate was set to Braak's intercept, i.e. 26.3°C (purple line).

4.3 Implication of altitudinal temperature change on altitudinal Holdridge life zone

LST maps generated based on the updated and Braak's altitudinal temperature lapse rate equations indicate temperature increase from 0.08 to 4.83 °C (Figure 8). Average of temperature increase in the window area of about 1.58°C was doubled from temperature increase at global scale of about 0.8 °C [26]. This implies to losses of montane and sub montane zones according to Holdridge life zone of about 7 km^2 (100%) and 727 km^2 (32.53%), respectively; and gain of basal zone of about 734 km^2 (211.77%); as shown in Figure 9.

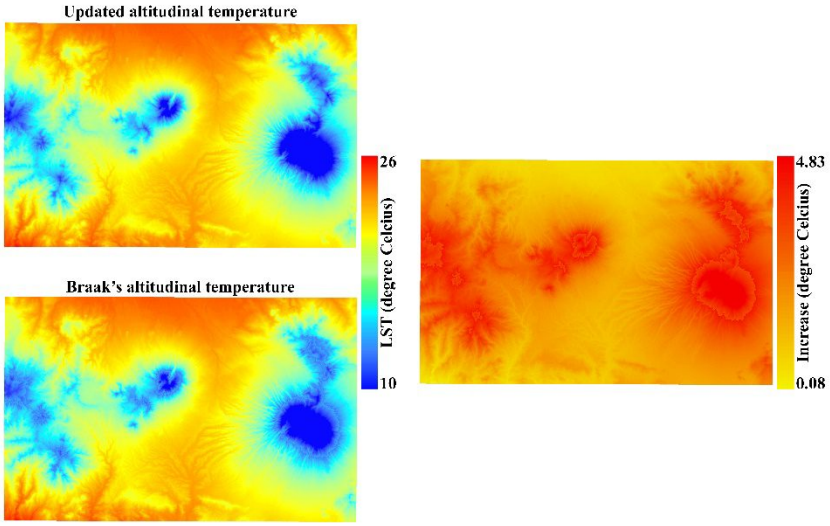

Figure 8. Updated altitudinal temperature (top left), Braak's altitudinal temperature (bottom left) and temperature departure of the updated altitudinal temperature from Braak (right).

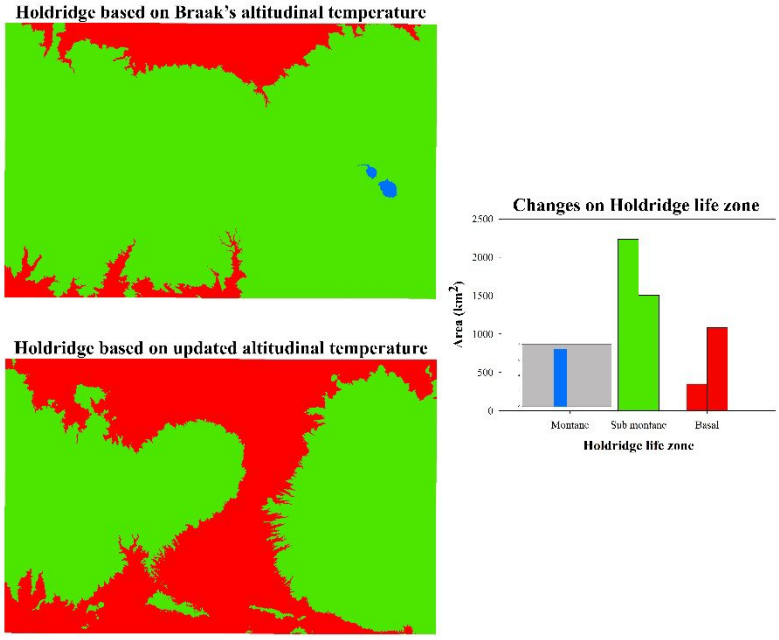

Figure 9. Changes on Holdridge altitudinal life zone as the implication of possible altitudinal temperature increase. In this case, 3 zones were identified in the window area: montane (blue), sub montane (green) and basal (red).

5. CONCLUSIONS

The results of this study suggest that Braak's equation on altitudinal temperature lapse rate should be revised, as the slope of the updated altitudinal temperature lapse rate equation decreased from 0.0016 to 0.0021°C.m^{-1}, as compared to Braak's equation, which indicate significant temperature increase. The results also suggest that temperature increase in the window area was identified of about 1.58°C, doubled from temperature increase at global scale of about 0.8 °C, which implies to losses of montane and sub montane zones according to Holdridge life zone of about 7 km^2 (100%) and 727 km^2 (32.53%), respectively; and gain of basal zone of about 734 km^2 (211.77%).

ACKNOWLEDGMENT

We would like to express our gratitude towards the International Partnership Programme (IPP) of the UK Space Agency through Ecometrica under Forests 2020 Project (https://ecometrica.com/forests2020) for the financial assistance.

REFERENCES

[1] Nasir, S.M., Afrasiyab, M. and Athar, M., "Application of Holdridge Life Zones (HLZ) in Pakistan," Pak. J. Bot., 47(SI), 359-366 (2015).
[2] Szelepcsényi, Z., Breuer, H. and Sümegi, P., "The climate of Carpathian Region in the 20th century based on the original and modified Holdridge life zone system," Cent. Eur. J. Geosci. 6(3), 293-307 (2014).
[3] Calef, M.P., McGuire, A.D., Epstein, H.E. Rupp, T.C. and Shugart, H.H., "Analysis of vegetation distribution in Interior Alaska and sensitivity to climate change using a logistic regression approach," J. Biogeogr. 32, 863–878 (2005).
[4] Lugo, A. E., Brown, S. L., Dodson, R., Smith, T. S. and Shugart, H.H., "The Holdridge life zones of the conterminous United States in relation to ecosystem mapping," J. Biogeogr. 26, 1025–1038 (1999).
[5] Prentice, I.C., Cramer, W., Harrison, S.P., Leemans, R., Monserud, R.A. and Solomon, A.M., "A global biome model based on plant physiology and dominance, soil properties and climate," J. Biogeogr. 19, 117–134 (1992).

[6] Dodson, R. and Marks, D., "Daily air temperature interpolated at high spatial resolution over a large mountainous region," Clim. Res. 8, 1-20 (1997).
[7] Gosciewski, D., "The effect of the distribution of measurement points around the node on the accuracy of interpolation of the digital terrain model," J. Geogr. Syst. 15, 513–535 (2013).
[8] Aguilar, F.J., Agüera, F., Aguilar, M.A. and Carvajal, F., "Effects of terrain morphology, sampling density, and interpolation methods on grid DEM accuracy," Photogramm. Eng. Remote Sens. 71 (7), 805–816 (2005).
[9] Marshall, J. and Plumb, R.A., [Atmosphere, Ocean, and Climate Dynamics: an Introductory Text. International Geophysics Series Volume 93], Elsevier Academic Press, 39-50 (2008).
[10] Barry, R.G. and Chorley, R.J., [Atmosphere, Weather and Climate, 8th Edition], Routledge, 89-90 (2003).
[11] Pyenson, L., [Empire of Reason: Exact Sciences in Indonesia, 1840-1940], Leiden, the Netherlands (1989).
[12] Suyamto, D., Prasetyo, L., Setiawan, Y., and Wijayanto, A., "Combining projective geometry modelling and spectral thresholding for automated cloud shadow masking in Landsat 8 imageries," Proc. 2017 European Modelling Symposium (EMS), Manchester (In Press).
[13] Nix, H.A., [The influence of climate on development of tropical forest areas], IUCN Publ. New Ser. 32, 66-87 (1975).
[14] Setyawan, A.D., "Distribusi dan kemelimpahan rubus di Gunung Lawu," BioSMART 1(2), 34–41 (1999).
[15] Suryanti, I., [Analisis Hubungan antara Sebaran Kekeringan Menggunakan Indeks Palmer dengan Karakteristik Kekeringan, Studi Kasus: Provinsi Banten], Undergraduate Thesis, Department of Geophysics and Meteorology, Faculty of Mathematics and Natural Sciences, Bogor Agricultural University, Bogor (2008).
[16] Sapta, S., Sulistyantara, B., Fatimah, I.S. and Faqih, A., "Geospatial approach for ecosystem change study of Lombok Island under the influence of climate change," Procedia Environ. Sci. 24, 165–173 (2015).
[17] Hidayati, R., [Application of Climate Information for Developing Early Warming Model and Controlling Dengue Fever Diseases Incidence in Indonesia], Doctoral Dissertation, Graduate School, Bogor Agricultural University, Bogor (2008).
[18] Aliffia, C., [Perencanaan Lanskap Laboratorium Lapang Pesantren Pertanian Darul Fallah, Ciampea, Bogor sebagai Tempat Wisata Pertanian], Undergraduate Thesis, Department of Landscape Architecture, Faculty of Agriculture, Bogor Agricultural University, Bogor (2010).
[19] Bahar, Y., [Rice Monitoring System Based on Modelling Approach], Master Thesis, Graduate School, Bogor Agricultural University, Bogor (2012).
[20] Arifianto, F., [The Characterization of Duku Production Levels and Disease Infestations Based on Rainfall in Jambi Province], Master Thesis, Graduate School, Bogor Agricultural University, Bogor (2017).
[21] Braak, C., [Het Klimaat van Nederlandisch-Indie, Deel I: Algemeene Hoofdstukken, English Summaries], Koninklijk Magnetisch en Meteorologisch Observatorium te Batavia, Verhandelingen 8, 123-158 (1929).
[22] Kuenzer, C., Zhang, J. and Dech, S., [Thermal Infrared Remote Sensing: Principles and Theoretical Background, In: P.S. Thenkabail (Ed.), Remote Sensing Handbook Volume I: Remotely Sensed Data Characterization, Classification, and Accuracies], CRC Press, Boca Raton, FL, USA, 259-275 (2016).
[23] Sobrino, J.A., Jime´nez-Mun˜oza, J.C. and Paolini, L., "Land surface temperature retrieval from LANDSAT TM 5," Remote Sens. Environ. 90, 434–440 (2004).
[24] USGS, "Using USGS Landsat 8 Product," <https://landsat.usgs.gov/using-usgs-landsat-8-product> (2016).
[25] Yu, X., Guo, X. and Wu, Z., "Land surface temperature retrieval from Landsat 8 TIRs — comparison between radiative transfer equation-based method, split window algorithm and single channel method," Remote Sens. 6, 9829-9852 (2014).
[26] Delsole, T., Tippett, M.K. and Shukla, J., "A significant component of unforced multidecadal variability in the recent acceleration of global warming," J. Climate 24(3), 909-926 (2011).